Size-Dependent Deformation and Adsorption Behavior of Carbon Monoxide, Hydrogen, and Carbon on Pyramidal Copper Clusters

W. Liu,[†,‡] Y. H. Zhao,[‡] E. J. Lavernia,*[,‡] and Q. Jiang*[,†]

Key Laboratory of Automobile Materials, Ministry of Education, and Department of Materials Science and Engineering, Jilin University, Changchun 130022, China, and Department of Chemical Engineering and Materials Sciences, University of California, Davis, California 95616

Received: January 16, 2008; Revised Manuscript Received: March 6, 2008

Density functional calculations are implemented to study the interaction of CO, H, and C with a sequential growth of Cu clusters with a special structure ($5 \leq n \leq 140$, where n is the number of atoms). The cohesive energy E_c and average bond length d_{ave} of the relaxed Cu clusters increase monotonically as the layer number of the clusters l increases. The adsorption energy E_{ad} values have a sequence of C/Cu < H/Cu < CO/Cu (adsorbate/substrate). The $E_{ad}(l)$ functions are found to be parabola-like for all adsorption systems, with the maximum values at $l = 5-6$ where $d_{ave} \approx 2.56$ Å, which is approximately equal to the atomic distance of Cu in bulk crystals. The binding strength between the adsorbate and substrate, or $-E_{ad}(l)$, is inversely proportional to their corresponding bond length d.

1. Introduction

Transition metal clusters have attracted considerable interest given their potential use as catalysts in many important reactions, such as oxidation and hydrogenation.[1–5] Recent experiments revealed that the activity of small metallic clusters is extremely sensitive to their sizes.[6–11] For instance, the Ir_4 cluster (the subscript denotes the number of atoms n) supported on γ-Al_2O_3 was found to be several times more efficient than the Ir_6 one for ethene hydrogenation under atmospheric pressure at 273–300 K.[7] As we all know, the properties of small clusters significantly differ from those of their corresponding bulk crystals, which can be attributed in part to the variation of the surface/volume ratio. This behavior has motivated investigators to propose new approaches to control catalysis by adjusting cluster size.[1] Thus, a systematic study of the properties of a sequential growth of clusters can provide important fundamental insight into the mechanisms that govern catalysis.[12,13] Experimental study of size-dependent catalytic behavior is challenging due to the difficulties associated with the preparation of uniform samples with varying dimensions.[6] Accordingly, computer simulation, in particular the density functional theory (DFT), has evolved as an essential tool in the study of catalytic behavior. In fact, DFT analysis offers distinct advantages in electronic structure determination, such as charge transfer and orbital hybridization. In essence, it is much easier to "prepare" a sequential growth of metal cluster "samples" for size effect analysis in the computer than it is in the laboratory.

There are numerous, often interrelated factors, such as temperature, pressure, morphology, and the characteristics of the substrate, that govern a catalytic reaction. Therefore, it is rather difficult to accurately describe the entire catalytic process.[14] Instead, it is useful to consider the simplified case of adsorption of a molecule or an atom on a cluster, which represents the first and essential step in surface catalysis.[13,15,16] Most prior studies addressed the central issue of how the cohesive energy E_c and adsorption energy E_{ad} values depend on the size of the cluster models.[17] On the basis of these studies, we know that in general, smaller clusters tend to be more active due to the large surface/volume ratio, and thus have larger E_c values.[18] However, calculated E_{ad} values often show considerable variations in magnitude, depending mostly on the size and shape of the cluster models. For instance, the E_{ad} values for H_2/Cu_n clusters are determined to be 0.65, 1.09, 1.43, 0.94, 1.04, 0.57, 0.63, 0.87, 0.96, 0.99, 0.75, 0.66, 0.76, and 0.81 eV for $n = 2, 3, \ldots, 15$, respectively.[3,13] No clear correlation between E_{ad} and n can be detected in the H_2/Cu_n system. Moreover, an odd–even vibrational phenomenon for E_{ad} values has been detected in H/Au and CO/Au systems,[19] the C/Pd system,[20] and the CO/Pd system with $55 \leq n \leq 146$, [17] which could be induced by an inadequate representation of the surface electronic structure in these cluster models.[21]

Prior works indicate that the atomic structures of the clusters change drastically with n where only ground-state structures of the substrates were considered.[3,13,17,19–24] Taking the methanol/Cu system as an example, Cu_2 is taken as a linear structure, Cu_3-Cu_6 are planar, while Cu_7-Cu_9 are three-dimensional clusters.[22] These results represent a departure from the well-accepted concept of "size dependence", which is that the structures of metals remain essentially unchanged.[16] Thus, studying the size effects on $E_c(n)$ and $E_{ad}(n)$ for a series of clusters with the same structure will provide new fundamental insight into the physical properties of nanoclusters, as well as their catalytic behavior under extreme conditions. Since no such adsorption systems have been systematically investigated with use of DFT calculations before, a series of pyramidal Cu clusters are established as a prototype in our study. In addition to the CO molecule, H and C atoms are selected as adsorbates, which are often used as probes on transition metal surfaces, while CO binding on small neutral Cu clusters has been recently studied for Cu_2-Cu_{13}.[23,24] Pyramidal clusters have attracted much scientific interest nowadays, partly due to their excellent emission properties when they are used as tips in field-emission electron spectroscopy.[25,26] In addition, the pyramidal clusters

* To whom correspondence should be addressed. E.J.L.: phone +1 530 752 0554, fax +1 530 752 8058, e-mail lavernia@ucdavis.edu. Q.J.: phone +86 431 85095371, fax +86 431 85095876, e-mail jiangq@jlu.edu.cn.
† Jilin University.
‡ University of California.

10.1021/jp800441w CCC: $40.75
Published on Web 04/30/2008

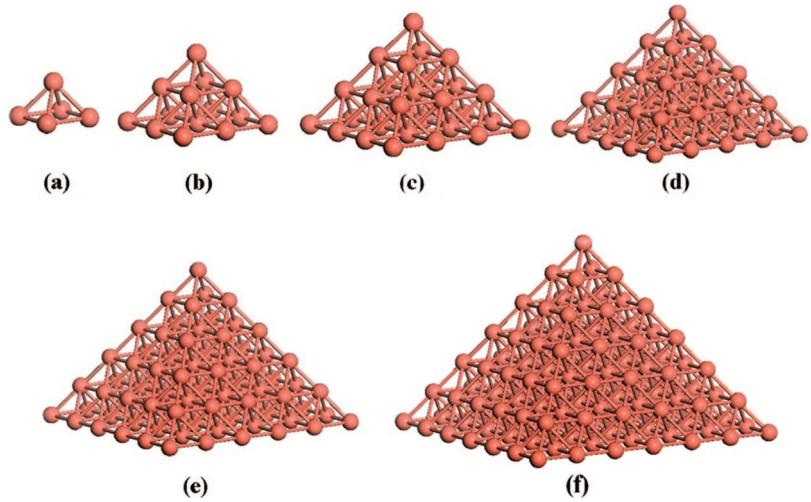

Figure 1. Clean pyramidal Cu clusters with l increases from 2 to 7.

have been observed in many growth processes of Cu, Ag, Fe, and Pt.[27–29] Therefore, a consideration on size effects at the electronic level will help us to understand the deformation and stability of single-atom electron sources.

In this contribution, six pyramidal Cu clusters with the number of layers l ranging from 2 to 7 are established. First-principles DFT calculations are performed to determine the geometry parameters, and size-dependent E_c and E_{ad} values for CO, H, and C on Cu clusters. It is found that the $E_{ad}(l)$ can be approximately considered as a function of the average bond length d_{ave}. In addition, the underlying relationships among the geometry, binding, and electric properties are discussed.

2. Simulation Details

The DFT framework used in this work is based on the DMol^3 code.[30,31] The double numerical basis set, augmented with polarization functions, is carried out to describe the valence electrons, with the core electrons considered with an effective core potential.[30] The relativistic effect is important for heavy elements like Cu, and thus DFT Semicore Pseudopotentials (DSPP) are taken throughout the paper.[32] The Fermi smearing is set to 0.005 hartree (Ha) (1 hatree = 27.2114 eV), and the global orbital cutoff is 4.0 Å. These settings yield a convergence tolerance of energy of 2.0×10^{-5} Ha, a maximum force of 0.004 Ha/Å, and a maximum displacement of 0.005 Å. The calculation results are very sensitive to the functionals. On one hand, although the local density approximation (LDA)[33] works better than the generalized gradient approximation (GGA) for slab properties,[34] it is not suitable for adsorption systems, because the E_{ad} values from LDA are numerically large by about 1.50 eV.[35] On the other hand, GGA with the Revised-Perdew−Burke−Ernzerhof (RPBE) function has been shown to be superior in the description of the energetics of atomic and molecular bonding to surfaces, which invokes a different mathematical form for the exchange energy enhancement factor.[35,36] In our previous work, the RPBE functional has been used to calculate the CO adsorption systems, and the obtained E_{ad} values are merely 5.02% lower than the experimental results on average.[37] Thus, RPBE is employed as the exchange-correlation functional throughout the paper. In addition, the spin-polarized calculations are employed to treat clusters with unpaired electrons.[13]

Six clusters with the same pyramidal structure are established first before the calculations, whose height h (or width w) ranges largely from 0.18 (or 0.36) to 1.08 (or 2.17) nm. As shown in Figure 1, n increases rapidly with l where $n = (1 + 2^2 + 3^2 + \cdots + l^2)$. In this contribution, $l_{max} = 7$ and thus $n_{max} = 140$. Before relaxation, the atoms are close-packed as in a Cu(111) surface, and thus the Cu−Cu distance $d = 2.56$ Å within the cluster.[38] It is discernible that a pyramidal model is composed of four Cu(111) surfaces and one Cu(100) surface. The lateral facets are an equilateral triangle, while the bottom one is a square. Since the geometry does not change with size, the symmetry retains C_{4v} for all of the clusters. After relaxation where all atoms are allowed to fully relax, the E_c values of clean Cu clusters are achieved by the following equation:

$$E_c = (E_{cluster} - nE_{atom})/n \quad (1)$$

where $E_{cluster}$ and E_{atom} denote the total energy of the cluster and that of a single Cu atom, respectively. n is the denominator and the unit of E_c is thus eV/atom. Two extreme conditions should be given, i.e., $E_c(n = 1) = 0$ and $E_c(n \rightarrow \infty) \approx E_{cbulk}$. Under this definition, $E_c < 0$.

There are seven types of possible atomic positions in a pyramidal structure: uppermost vertex (the coordination number CN = 4), bottom vertices (CN = 3), lateral edges (CN = 7), bottom edges (CN = 5), lateral facets (CN = 9), bottom facets (CN = 8), and interior (CN = 12 as the condition of bulk Cu crystals). In chemistry, dissociation energy E_{dis} is defined as the required energy to break all the bonds around an atom, which equals the bond energies for a diatomic molecule.[39] Since the models are related to the tips, the stability of the uppermost vertex atom is evaluated by estimating its E_{dis}. Taking the 5-layer cluster as an example, the vertex atom moves "infinitely" far way to break the four bonds connected to the second layer, and the calculated $E_{dis} = 2.60$ eV. Considering the E_{dis} of F_2 is only 1.65 eV (i.e., the lowest energy to separate an F_2 molecule into two F atoms),[40] the uppermost vertex atom here is quite stable. In fact, previous experiments have proved that a single atom ended nanopyramid is the thermodynamically stable structure during the heating process.[25,41] A Cu cluster owns numerous adsorption possibilities if all the "atop", "bridge", and "hollow" sites are also considered. To render the E_{ad} values comparable, all adsorbates are placed on the Cu atom at the uppermost vertex. As shown in Figure 2, three adsorption models of CO, H, and C on a 5-layer Cu substrate will be considered. Among them, the initial C−O distance is set to 1.13 Å in light of available experimental data.[42] After relaxation, four Cu atoms at the

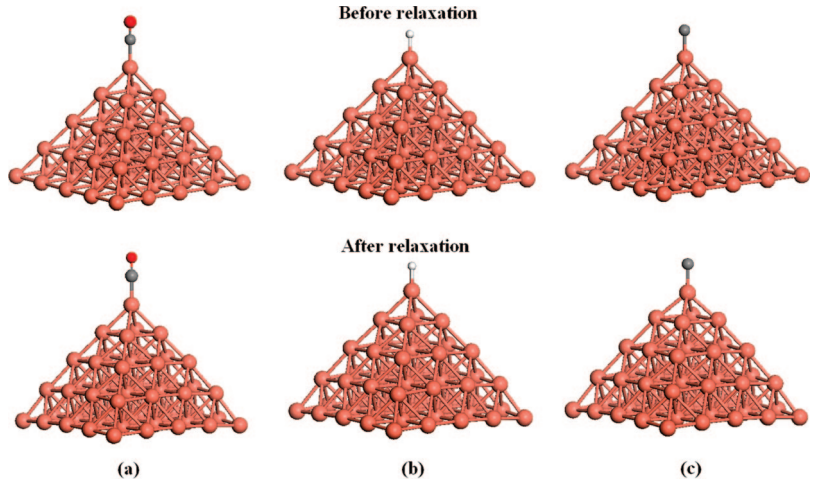

Figure 2. Adsorption models of the 5-layer Cu cluster: (a) CO/Cu, (b) H/Cu, and (c) C/Cu. The plots both before and after relaxation are depicted. The sphere shows Cu, O, C, and H atom from the largest to the smallest in sequence.

TABLE 1: Computed Cohesive Energy Values (E_c in eV/atom) and Geometric Parameters (Height h and Width w in Å, Apex Angle θ in deg, and the Distance between the First and Second Layer d_{12} in Å) for Clean Cu Clusters[a]

L	n	E_c	h_0[b]	h_1[c]	h_2[c]	$\lvert\Delta h\rvert$[d]	w_0	w_1	$\lvert\Delta w\rvert$[e]	θ_0	θ_1	d_{12}
2	5	1.42	1.81	1.61	1.61	0	3.62	3.53	0.09	90.00	95.23	1.61
3	14	1.96	3.62	3.61	3.51	0.10	7.23	6.89	0.34	90.00	91.60	1.73
4	30	2.24	5.42	5.26	5.38	0.12	10.86	10.38	0.48	90.00	96.31	1.66
5	55	2.40	7.23	7.12	7.30	0.18	14.46	13.76	0.70	90.00	94.95	1.68
6	91	2.50	9.04	8.86	9.21	0.35	18.08	17.22	0.86	90.00	96.43	1.66
7	140	2.58	10.84	10.66	11.10	0.44	21.70	20.62	1.08	90.00	96.29	1.66

[a] The meaning of each parameter can be seen in Figure 3. [b] Subscript "0" indicates h value in the unrelaxed cluster, as shown in Figure 6a. [c] Subscripts "1" and "2" indicate the h value in the fully relaxed clusters, as shown in Figure 6b. [d] $|\Delta h| = |h_2 - h_1|$ shows the rumple degree of the bottommost layer. [e] $|\Delta w| = |w_1 - w_0|$ shows the contraction degree of the bottommost layer.

bottom vertices deform most severely because their CN value is the smallest among all Cu atoms in the cluster. E_{ad} is often introduced to describe the binding strength between the gas-phase molecule (or atom) and the metals, which is determined by

$$E_{ad} = E_t - (E_{cluster} + E_{gas}) \quad (2)$$

where the subscripts "t" and "gas" denote the total amount of the considered syste, and the corresponding "free" CO molecules, or H and C atoms.

3. Results and Discussion

Table 1 shows the calculated $E_c(l)$ values and geometric parameters of relaxed Cu clusters. $E_c(l) = -1.42, -1.96, -2.24, -2.40, -2.50$, and -2.58 eV/atom when $2 \le l \le 7$, respectively. In terms of the results, $E_c(l)$ is a function of the surface bond deficit and decreases monotonically as l or n increases. This differs from an oscillating behavior of $E_c(n)$ values for Cu_7-Cu_{12},[43] where adding or subtracting one atom in the cluster could lead to evident change of the total broken bond numbers, and thus the E_c values of the clusters vibrate.[44] Since the stability of a cluster increases with decreasing of E_c, larger clusters are more stable. The above results differ from previous results from DFT calculations,[13,43,45,46] such as $E_c = -1.63$ and -2.26 eV/atom respectively for Cu_5 (triangular) and Cu_{14} (icosahedral),[13] since we have fixed the structure of the clusters.

To describe the deformation states of clean Cu clusters, some parameters are determined and shown in Table 1 and Figure 3. $h_0 = 1.81 \times (l - 1)$ indicates the height of the cluster before relaxation, as shown in Figure 3a. For the relaxed cluster, h_1 (or h_2) shows the vertical distance between the uppermost vertex and the central atom (or the bottom vertices) in the bottommost layer, see Figure 3b. When $l > 3$, the former (or the latter) has the smallest (or the largest) value between the uppermost vertex and the bottom layer. This renders an arc shape of each layer. In Table 1, $h_1 < h_2$ when $l > 3$. When $l = 2$ and 3, the above definitions for h_1 and h_2 are not fully satisfied. For $l = 2$, $h_1 = h_2 = 1.61$ Å since they both indicate the same atomic distance, see Figure 1a. For the case of $l = 3$, $h_1 = 3.61 > h_2 = 3.51$ Å, it is not the atom at the center of the bottom facet, but the one at the bottom edge that has the smallest vertical distance. In Table 1, $|\Delta h|$ values increase monotonically from 0 to 0.44 Å as l increases. In addition, $h_0 > h_1$ and $h_0 > h_2$ when $l = 2-4$. $h_2 > h_0 > h_1$ when $l \ge 5$, however. All these phenomena imply that the bottom layer deforms or rumples more severely as l increases.

As shown in Figure 3, w shows the largest width of the clusters, which is also the length of the bottommost layer. Δw is defined as the difference between w_1 and w_0. In Table 1, $w_1 < w_0$ and thus $\Delta w < 0$ in all cases, denoting the contraction of the bottom facets of clusters inward after a full relaxation. This response is not unexpected because clusters prefer to be quasispherical shapes to minimize their surface/volume ratio. They may change from icosahedron, to truncated decahedron, to truncated octahedron when growing in size.[47] In fact, it is discernible that four corners in the top view of Figure 3b are not as sharp as before. Similar to $|\Delta h|$, $|\Delta w| = |w_1 - w_0|$ increases as l increases, which describes the extent of deformation along the horizontal axis. As shown in Figure 3a, the apex angle $\theta_0 \equiv 90°$ is due to the same pyramidal structure. Interestingly, θ_0 increases following a relaxation and shows an obvious odd–even oscillation. The θ_1 value of the odd-layer

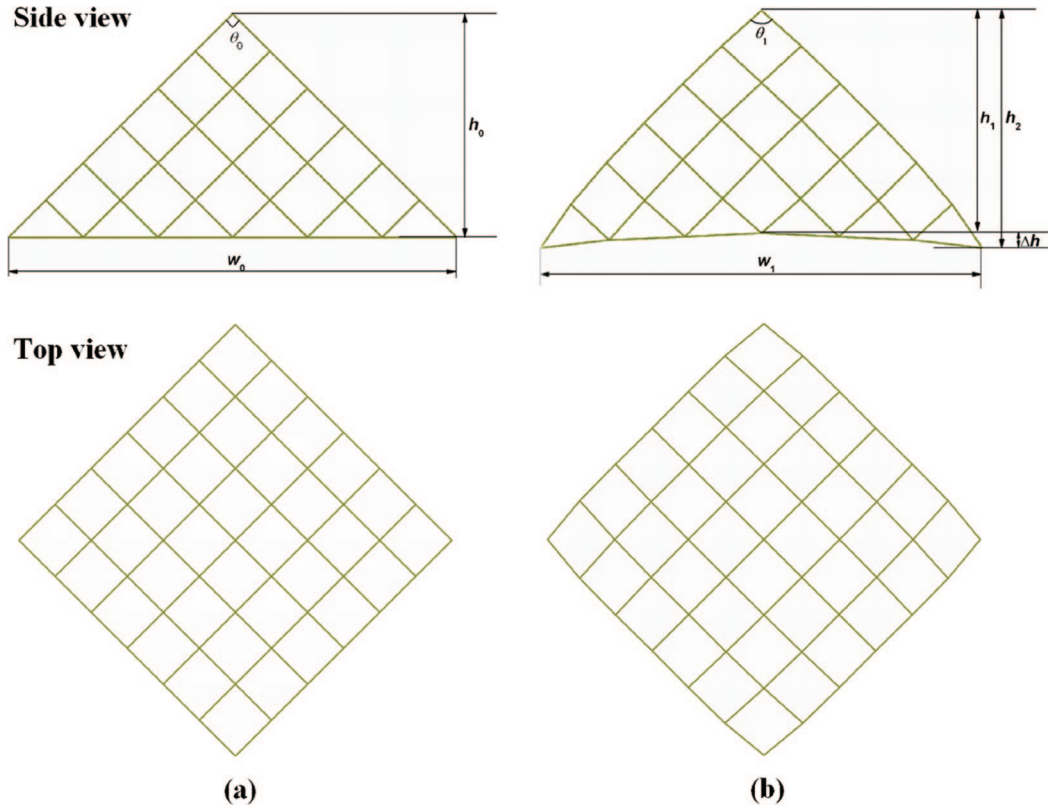

Figure 3. Schematic plots for deformation of clean Cu clusters: (a) before relaxation and (b) after relaxation.

TABLE 2: Computed Adsorption Energy E_{ad} Values (in eV), and Bond Length d (in Å) for CO/Cu, H/Cu, and C/Cu Adsorption Systems, as Well as the Average Bond Length d_{ave} Values of Clean Cu Clusters

l	$-E_{ad1}$[a]	d_{1C-Cu}	d_{1C-O}	$-E_{ad2}$[a]	d_{2H-Cu}	$-E_{ad3}$[a]	d_{3C-Cu}	d_{ave}	Δd_{ave}[b]
2	1.72	1.79	1.15	2.34	1.50	2.91	1.71	2.45	0.11
3	1.18	1.81	1.15	2.30	1.50	2.69	1.69	2.50	0.06
4	0.94	1.83	1.15	2.07	1.51	2.50	1.72	2.54	0.02
5	0.92	1.84	1.15	2.09	1.51	2.24	1.77	2.56	0
6	1.01	1.82	1.15	1.93	1.51	2.33	1.76	2.57	0.01
7	1.03	1.82	1.15	2.18	1.50	2.56	1.76	2.58	0.02

[a] The subscripts "1", "2", and "3" indicate the adsorption systems of CO, H, and C on Cu clusters, respectively. [b] $\Delta d_{ave} = |d_{ave} - d_{bulk}|$, where $d_{bulk} = 2.56$ Å is the nearest atomic distance of bulk Cu.

cluster listed in Table 1 is lower than its neighboring even-layer ones. Some layer−layer separations in the clusters are also measured as the number of layers increases. When l increases from 2 to 7, the layer distances between the first and second layer d_{12} are measured, which are 1.61, 1.73, 1.66, 1.68, 1.66, and 1.66 Å, respectively. Differing from θ_1, the d_{12} value of the even-layer cluster is lower than its neighboring odd-layer ones. This implies that a larger θ_1 corresponds to a smaller d_{12}. On the other hand, each layer-to-layer distance of the 7-layer cluster is determined. After full relaxation, the average layer distances (since most layers are not flat) from up to down are 1.66, 1.71, 1.82, 1.83, 1.92, and 1.98 Å, respectively. Since the unrelaxed layer distance is 1.81 Å, the first three layers contract, while the bottom four layers expand due to the large rumple.

The calculated E_{ad} values, and the corresponding geometry parameters, for CO, H, and C on Cu clusters are given in Table 2. For the CO/Cu adsorption system, 2-layer Cu has the lowest E_{ad} value and thus exhibits the largest adsorption ability. Then, E_{ad} increases as l increases from 3 to 5, where $E_{ad1}(l) = -1.18$, -0.94, and -0.92 eV, respectively. However, E_{ad1} values decrease to -1.01 and -1.03 eV when $l = 6$ and 7. In general, the binding strength, or $-E_{ad}$, is inversely proportional to its corresponding d value between the adsorbate and the substrate.[24] This is our case shown in Table 2 where the trend of $d_{1C-Cu} \propto E_{ad1}$. Thus, our "abnormal" E_{ad} value corresponds to their corresponding d_{1C-Cu} values. Comparing with the experimental results, $d_{C-Cu} = 1.91$ Å for CO on Cu(111) surfaces[48] is much larger than our d_{1C-Cu} values, which confirms that CO binds more strongly on small clusters. In addition, the d_{1C-O} values slightly increase from 1.13 to 1.15 Å for all clusters in Table 2. It is well-known that the binding between CO and low-index Cu surfaces is weak.[49] Recent experimentally determined heat of adsorption for the CO/Cu(111) system was reported to be -0.49 eV,[50] which is much larger than the E_{ad1} values listed in Table 2. It is imperative to note that it is not quite reasonable to compare the present results with those obtained from experiments. This is because only the end-on coordination (CN = 4) is considered here, while CN ≡ 9 for each surface atom in the (111) surface in experiments. Obviously, the adsorption ability would significantly decrease if all the surface atoms in the cluster are considered. It is worth noting that our E_{ad} value for CO on the 5-atom pyramidal Cu ($l = 2$) is 52.99% lower than the $E_{ad} = -1.17$ eV value for CO on ground-state Cu_5.[23] This is because an unstable cluster is more "eager" to adsorb small molecules to lower its free energy.

Similar trends of $E_{ad}(l)$ can also be found for the H/Cu and C/Cu systems in Table 2. For the former, $E_{ad2}(l) = -2.34$, -2.30, -2.07, -2.09, -1.93, and -2.18 eV when $l = 2-7$, respectively. d_{2H-Cu} increases from 1.50 to 1.51 Å when $2 \le l \le 6$. Then, it decreases to 1.50 Å again when $l = 7$, which corresponds to a function of $E_{ad2}(l)$. On the other hand, the maximal value of C/Cu occurs at $l = 5$, where $E_{ad3}(l) = -2.91$, -2.69, -2.50, -2.24, -2.33, and -2.56 eV, respectively. As shown in Figure 4, the charts of E_{ad} with respect to l are

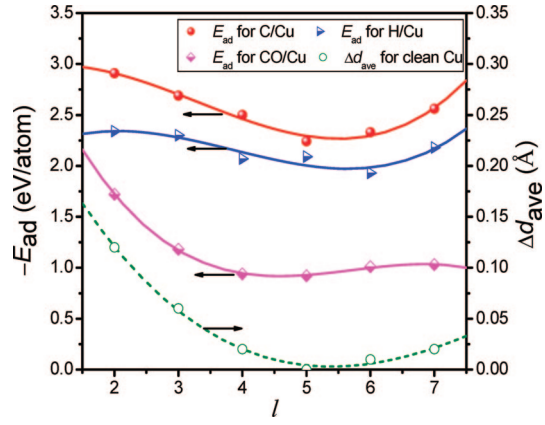

Figure 4. Plots of E_{ad} and Δd_{ave} values with respect to l, where the discrete data are fitted by a third-order exponential function.

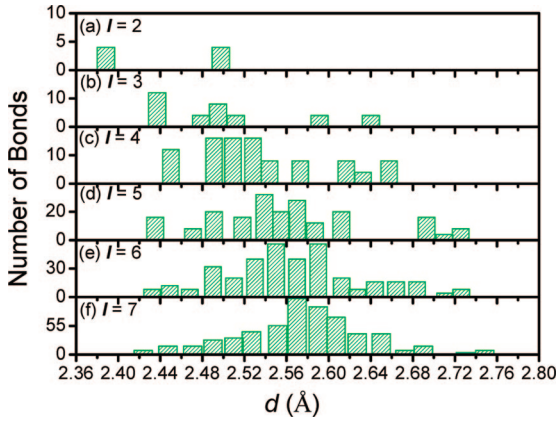

Figure 5. The distributions of the bond length d for fully relaxed Cu clusters with $l = 2-7$; their corresponding average bond length d_{ave} values are listed in Table 2.

depicted, where the discrete data are fitted by a third-order exponential function. It is discernible that the curves are parabola-like for all three systems, where the inflection appears at about $l = 5-6$. In this figure, the E_{ad} value has a sequence of C < H < CO, which implies that the interaction between CO and Cu is the weakest. This is understandable since the activity of the CO molecule should be much lower than that of free atoms. On the other hand, the C atom ($2s^2 2p^2$) has more empty orbitals than H ($1s^1$), and thus can accept more charges from Cu.

To explain the parabolic $E_{ad}(l)$ functions, the bond distributions of the clean Cu clusters are further investigated and shown in Figure 5. In Figure 5a, there are totally eight bonds in a 2-layer cluster, which are located at 2.39 and 2.50 Å, respectively. Then, d increases regularly as l increases from 2 to 4. However, the shortest bond of the 5-layer cluster with $d = 2.43$ Å is even shorter than that of a 4-layer cluster, which relates to the four atoms at bottom vertices. In addition, the results show that the largest bond lengths of the 5-layer cluster also appear between the fourth and the bottommost layers. Thus, it is clear that the bottom layer deforms the most after a relaxation. Similar bond distributions can be found in parts e and f of Figure 5 for clusters with $l = 6$ and 7. From the above analysis, the structures change so severely that the precondition of "same structure" may not be preserved for larger clusters. This is presumably a reason why the $E_{ad}(l)$ function is not monotonic with $l > 5$.

Since too many atoms and bonds exist in a cluster, for simplicity, their corresponding average bond length d_{ave} values are calculated and listed in Table 2. Take the simplest 2-layer

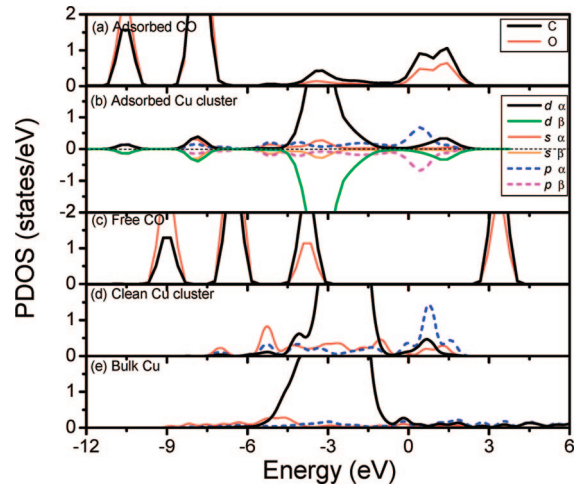

Figure 6. PDOS plots of CO on a 4-layer Cu cluster: (a) adsorbed CO, (b) adsorbed Cu cluster, where both the spin-up (α) and spin-down (β) states are depicted, (c) free CO, (d) clean Cu cluster, and (e) bulk Cu. The Fermi level is located at 0 eV.

cluster as an example, $d_{ave} = (4 \times 2.39 + 4 \times 2.50)/8 = 2.45$ Å. From this table, d increases regularly from 2.45 to 2.58 Å as l increases from 2 to 7. Notably, the nearest atomic distance d_{bulk} of the bulk Cu crystal is 2.56 Å.[38] This makes $l = 5$ quite special since $d_{ave}(5) = 2.56$ Å. In Table 2, $d_{ave} < 2.56$ Å when $l < 5$, while $d_{ave} > 2.56$ Å when $l > 5$. Since the (111) surface owns the weakest adsorption ability, 2.56 Å can be selected as a reference. As shown in Figure 4, the chart of $\Delta d_{ave} = |d_{ave} - 2.56|$ with respect to l is depicted. It can be seen that the $\Delta d_{ave}(l)$ function is also parabolic, which has the same trend as those of $E_{ad}(l)$. This may be another reason why $l = 5$ is an inflection in our E_{ad} calculations.

To look into the orbital hybridization conditions, the partial density of states (PDOS) charts for CO on 4-layer Cu are chosen as an example and shown in Figure 6. For comparison purposes, plots of the free CO molecule, clean Cu cluster, and bulk Cu crystal are also depicted there. For a free CO, the orbitals of 4σ, 1π, 5σ, and $2\pi^*$ are localized at about −8.99, −6.57, −3.77, and 3.47 eV, respectively. Comparing with Figure 6c, the states of adsorbed CO move largely to a lower energy range, where the 4σ orbital is still localized, while the 5σ and 1π orbitals broaden and dominate the interaction, see Figure 6a. Both the contributions from spin-up (α) and spin-down (β) states for adsorbed Cu are plotted in Figure 6b, from which it is discernible that β is identical with α except for the spin direction. This is consistent with the conditions of the HOMO (highest occupied molecular orbitals) and LUMO (lowest unoccupied molecular orbitals) orbitals for CO on small Cu clusters.[24] Comparing parts a of Figure 6 with part b, not only d, but also s and p states of Cu hybridize strongly with those of adsorbed CO. Thus, a new bond is formed between C and Cu due to the charge transfer between them. The states of the Cu cluster after adsorption move left in comparison with those of the clean Cu cluster, see Figure 6d. This implies that the stability increases when small molecules are adsorbed. Notably, the band of bulk Cu is dominated by the d orbital, and a very weak p state can be seen in Figure 6e. Interestingly, large contributions from s and p orbitals can be detected in the PDOS plot for the clean Cu cluster. Among them, the p state becomes especially intensive for the oribitals above the Fermi level, as shown in Figure 6d. Thus, the Cu cluster has a stronger adsorption ability than that of the bulk Cu crystal where the former owns more empty orbitals to accept the charges from the CO molecule. Obviously,

the above discussions about the electronic properties are suitable for the PDOS plots of H/Cu and C/Cu adsorption systems.

Blyholder's model is frequently used to describe the interaction between CO and metals.[51] However, donation and back-donation occurs simultaneously in this bonding scheme, and thus the specific net charge transfer direction cannot be predicted.[24] Thus, Hirshfeld charge analysis is employed here to investigate the transfer direction of net charges. If one considers a 5-layer Cu cluster as an example, adsorbed C and O decreases from +0.0764 and −0.0764 to +0.0589 and −0.0901 respectively, while Cu at the uppermost vertex increases from +0.0097 to +0.0622. This implies that net charge transfers from Cu to CO after adsorption. Similarly, results show that net charges transfer from Cu to H and C, where adsorbed H (or C) decreases from 0 to −0.2305 (or −0.2182), while Cu increases from +0.0097 to +0.0146 (or +0.0217). Similar results were achieved for the CO/Ir(111) surface,[37] C_2H_2 absorbed on low-index Cu surfaces,[52] and the dissociative chemisorption of H_2/Cu clusters.[13] Interestingly, an opposite charge transfer direction would be observed if Mulliken charge analysis is employed, where CO increases from 0 to +0.201, while Cu decreases from −0.036 to −0.155. Note that Mulliken population distribution cannot give the correct direction of charge flow, because of its indiscriminative division scheme to divide the charges at the middle of a bond.[53]

4. Conclusions

In conclusion, DFT calculations with the DSPP core treatment method are employed to study the deformation of pyramidal Cu clusters, as well as their interactions with three adsorbates of CO, H, and C. Clusters deform more and more severely as size increases, where the θ values of relaxed clusters show an obvious odd–even vibration. For CO and C on Cu clusters, the $E_{ad}(l)$ functions increase monotonically as l increases from 2 to 5, and then decline from 5 to 7. A similar trend is also observed in the H/Cu system, but the critical layer is not 5 but 6. The above results might be attributed to the large deformation when $l > 5$, and to their corresponding Δd_{ave} values.

Acknowledgment. Liu and Jiang acknowledge financial support from the National Key Basic Research and Development Program of China (Grant No. 2004CB619301) and the "985 Project" of Jilin University. Zhao and Lavernia would like to acknowledge support by the Office of Naval Research of the USA (Grant Nos. N00014-04-1-0370 and N00014-08-1-0405) with Dr. Lawrence Kabacoff as program officer.

References and Notes

(1) Xu, Z.; Xiao, F.-S.; Purnell, S. K.; Alexeev, O.; Kawi, S.; Deutsch, S. E.; Gates, B. C. *Nature* **1994**, *372*, 346.
(2) Jacobs, K.; Zaziski, D.; Scher, E. C.; Herhold, A. B.; Alivisatos, A. P. *Science* **2001**, *293*, 1803.
(3) Guvelioglu, G. H.; Ma, P.; He, X.; Forrey, R. C.; Cheng, H. *Phys. Rev. Lett.* **2005**, *94*, 026103.
(4) Tada, M.; Sasaki, T.; Iwasawa, Y. *J. Catal.* **2002**, *211*, 496.
(5) Safonova, O. V.; Tromp, M.; van Bokhoven, J. A.; de Groot, F. M. F.; Evans, J.; Glatzel, P. *J. Phys. Chem. B* **2006**, *110*, 16162.
(6) Li, F.; Gates, B. C. *J. Phys. Chem. C* **2007**, *111*, 262.
(7) Argo, A. M.; Odzak, J. F.; Gates, B. C. *J. Am. Chem. Soc.* **2003**, *125*, 7107.
(8) Bergamaski, K.; Pinheiro, A. L. N.; Teixeira-Neto, E.; Nart, F. C. *J. Phys. Chem. B* **2006**, *110*, 19271.
(9) Semagina, N.; Renken, A.; Kiwi-Minsker, L. *J. Phys. Chem. C* **2007**, *111*, 13933.
(10) Panigrahi, S.; Basu, S.; Praharaj, S.; Pande, S.; Jana, S.; Pal, A.; Ghosh, S. K.; Pal, T. *J. Phys. Chem. C* **2007**, *111*, 4596.
(11) Deng, J.-P.; Shih, W.-C.; Mou, C.-Y. *ChemPhysChem.* **2005**, *6*, 2021.
(12) Forrey, R. C.; Guvelioglu, G. H.; Ma, P.; He, X.; Cheng, H. *Phys. Rev. B* **2006**, *73*, 155437.
(13) Guvelioglu, G. H.; Ma, P.; He, X.; Forrey, R. C.; Cheng, H. *Phys. Rev. B* **2006**, *73*, 155436.
(14) Schubert, M. M.; Hackenberg, S.; van Veen, A. C.; Muhler, M.; Plzak, V.; Behm, R. J. *J. Catal.* **2001**, *197*, 113.
(15) Reboredo, F. A.; Galli, G. *J. Phys. Chem. B* **2006**, *110*, 7979.
(16) Lu, H. M.; Wen, Z.; Jiang, Q. *Chem. Phys.* **2005**, *309*, 303.
(17) Yudanov, I. V.; Sahnoun, R.; Neyman, K. M.; Rösch, N. *J. Chem. Phys.* **2002**, *117*, 9887.
(18) Jiang, Q.; Li, J. C.; Chi, B. Q. *Chem. Phys. Lett.* **2002**, *366*, 551.
(19) Phala, N. S.; Klatt, G.; Van Steen, E. *Chem. Phys. Lett.* **2004**, *395*, 33.
(20) Neyman, K. M.; Inntam, C.; Gordienko, A. B.; Yudanov, I. V.; Rösch, N. *J. Chem. Phys.* **2005**, *122*, 174705.
(21) Hermann, K.; Bagus, P. S.; Nelin, C. J. *Phys. Rev. B* **1987**, *35*, 9467.
(22) Hsu, W.-D.; Ichihashi, M.; Kondow, T.; Sinnott, S. B. *J. Phys. Chem. A* **2007**, *111*, 441.
(23) Cao, Z.; Wang, Y.; Zhu, J.; Wu, W.; Zhang, Q. *J. Phys. Chem. B* **2002**, *106*, 9649.
(24) Poater, A.; Duran, M.; Jaque, P.; Toro-Labbé, A.; Solà, M. *J. Phys. Chem. B* **2006**, *110*, 6526.
(25) Fu, T. Y.; Cheng, L. C.; Nien, C. H.; Tsong, T. T. *Phys. Rev. B* **2001**, *64*, 113401.
(26) Kuo, H. S.; Hwang, I. S.; Fu, T. Y.; Wu, J. Y.; Chang, C. C.; Tsong, T. T. *Nano Lett.* **2004**, *4*, 2379.
(27) Botez, C. E.; Miceli, P. F.; Stephens, P. W. *Phys. Rev. B* **2001**, *64*, 125427.
(28) Ernst, H.-J.; Fabre, F.; Folkerts, R.; Lapujoulade, J. *Phys. Rev. Lett.* **1994**, *72*, 112.
(29) Maroutian, T.; Douillard, L.; Ernst, H.-J. *Phys. Rev. B* **2001**, *64*, 165401.
(30) Delley, B. *J. Chem. Phys.* **1990**, *92*, 508.
(31) Delley, B. *J. Chem. Phys.* **2000**, *113*, 7756.
(32) Delley, B. *Phys. Rev. B* **2002**, *66*, 155125.
(33) Ceperley, D. M.; Alder, B. J. *Phys. Rev. Lett.* **1980**, *45*, 566.
(34) Mattsson, A. E.; Schultz, P. A.; Desjarlais, M. P.; Mattsson, T. R.; Leung, K. *Modell. Simul. Mater. Sci. Eng.* **2005**, *13*, R1.
(35) Hammer, B.; Hansen, L. B.; Nørskov, J. K. *Phys. Rev. B* **1999**, *59*, 7413.
(36) Mavrikakis, M.; Rempel, J.; Greeley, J.; Hansen, L. B.; Nørskov, J. K. *J. Chem. Phys.* **2002**, *117*, 6737.
(37) Liu, W.; Zhu, Y. F.; Lian, J. S.; Jiang, Q. *J. Phys. Chem. C* **2007**, *111*, 1005.
(38) King, H. W. *Physical Metallurgy*; Cahn, R. W., Haasen, P., Eds.; North-Holland Physics Publishing: Amsterdam, The Netherlands, 1983.
(39) McNaught, A. D.; Wilkinson, A. *Compendium of Chemical Terminology*, The Gold Book, 2nd ed.; Blackwell Science: Oxford, UK, 1997.
(40) Huber, K. P.; Herzberg, G. L. *Molecular Spectra and Molecular Structure IV. Constants of Diatomic Molecules*; Van Nostrand Reinhold: New York, 1979.
(41) Ishikawa, T.; Urata, T.; Cho, B.; Rokuta, E.; Oshima, C.; Terui, Y.; Saito, H.; Yonezawa, A.; Tsong, T. T. *Appl. Phys. Lett.* **2007**, *90*, 143120.
(42) Lide, D. R., Ed. *CRC Handbook of Chemistry and Physics*, 81th ed.; CRC Press: Boca Raton, FL, 2000.
(43) Fernández, E. M.; Soler, J. M.; Garzón, I. L.; Balbás, L. C. *Phys. Rev. B* **2004**, *70*, 165403.
(44) Schmidt, M.; Haberland, H. *C. R. Phys.* **2002**, *3*, 327.
(45) Yang, M.; Jackson, K. A.; Koehler, C.; Frauenheim, T.; Jellinek, J. *J. Chem. Phys.* **2006**, *124*, 024308.
(46) Jaque, P.; Toro-Labbé, A. *J. Chem. Phys.* **2002**, *117*, 3208.
(47) Baletto, F.; Ferrando, R. *Rev. Mod. Phys.* **2005**, *77*, 371.
(48) Moler, E. J.; Kellar, S. A.; Huff, W. R. A.; Hussain, Z.; Chen, Y.; Shirley, D. A. *Phys. Rev. B* **1996**, *54*, 10862.
(49) Sakong, S.; Mosch, C.; Gross, A. *Phys. Chem. Chem. Phys.* **2007**, *9*, 2216.
(50) Vollmer, S.; Witte, G.; Wöll, C. *Catal. Lett.* **2001**, *77*, 97.
(51) Blyholder, G. *J. Phys. Chem.* **1964**, *68*, 2772.
(52) Liu, W.; Lian, J. S.; Jiang, Q. *J. Phys. Chem. C* **2007**, *111*, 18189.
(53) Chen, L.; Cooper, A. C.; Pez, G. P.; Cheng, H. *J. Phys. Chem. C* **2007**, *111*, 5514.

JP800441W